PARKINSON'S DISEASE

Slow-wave sleep affects synucleinopathy and regulates proteostatic processes in mouse models of Parkinson's disease

Marta M. Morawska[1,2], Carlos G. Moreira[1,3], Varun R. Ginde[1], Philipp O. Valko[1], Tobias Weiss[1], Fabian Büchele[1], Lukas L. Imbach[1], Sophie Masneuf[1], Sedef Kollarik[1,2], Natalia Prymaczok[4], Juan A. Gerez[4], Roland Riek[4], Christian R. Baumann[1,2,5]†, Daniela Noain[1,2,5]*†

Slow-wave sleep (SWS) modulation in rodent models of Alzheimer's disease alters extracellular amyloid burden. In Parkinson's disease (PD), SWS appears to be closely linked with disease symptoms and progression. PD is characterized by damaging intracellular α-synuclein (αSyn) deposition that propagates extracellularly, contributing to disease spread. Intracellular αSyn is sensitive to degradation, whereas extracellular αSyn may be eliminated by glymphatic clearance, a process increased during SWS. Here, we explored whether long-term slow-wave modulation in murine models of PD presenting αSyn aggregation alters pathological protein burden and, thus, might constitute a valuable therapeutic target. Sleep-modulating treatments showed that enhancing slow waves in both VMAT2-deficient and A53T mouse models of PD reduced pathological αSyn accumulation compared to control animals. Nonpharmacological sleep deprivation had the opposite effect in VMAT2-deficient mice, severely increasing the pathological burden. We also found that SWS enhancement was associated with increased recruitment of aquaporin-4 to perivascular sites, suggesting a possible increase of glymphatic function. Furthermore, mass spectrometry data revealed differential and specific up-regulation of functional protein clusters linked to proteostasis upon slow wave–enhancing interventions. Overall, the beneficial effect of SWS enhancement on neuropathological outcome in murine synucleinopathy models mirrors findings in models of Alzheimer. Modulating SWS might constitute an effective strategy for modulating PD pathology in patients.

INTRODUCTION

The close relationship between neurodegenerative disease and sleep has gained increasing attention in recent years. It is now widely recognized that sleep-wake disturbances are present in virtually every brain disorder, including Parkinson's disease (PD) (*1–3*), which is often heralded by rapid eye movement (REM) sleep behavior disorder (*4*). Conversely, recent research has strongly suggested that poor sleep can exacerbate disease expression and progression (*5–10*), raising the possibility of sleep modulation as a disease-modifying intervention. The most solid evidence stems from the study of Alzheimer's disease (AD). In 2009, a landmark study observed that enhanced sleep reduced amyloid-β plaque deposition in a rodent model of AD, whereas sleep restriction had an opposite effect (*5*). Clinical studies have corroborated these findings; self-reported poor sleep in healthy elderly people is related to greater amyloid-β burden (*8*), and studies of the cerebrospinal fluid (CSF) of healthy adults suggest that acute slow-wave sleep (SWS) disruption can increase amyloid-β concentrations, whereas multiple nights with poor sleep increase tau. These results indicate a functional role of sleep in protein turnover (*6, 9*). In PD, both light therapy (*11*) and

SWS sleep enhancement (SE) with sodium oxybate reduced excessive daytime sleepiness (*12*). Moreover, SWS appears to be inversely correlated with disease progression and thus to exert a potential neuroprotective effect (*13*). The mechanisms underlying such putative disease-modifying properties of SWS remain unclear. Recent evidence has suggested the presence of a glymphatic system in the human brain, which could be responsible for clearing waste, including accumulated proteins (*14, 15*). Other studies suggest that SE increases glymphatic clearance in both mice and human brains (*16, 17*), resulting in decreased protein aggregation. Although glymphatic function has been primarily associated with SWS (*16, 18*), recent studies have also shown a potential role of REM sleep oscillations in neurovascular coupling (*19, 20*), possibly affecting glymphatic activity (*21*). Conversely, sleep deprivation (SD) has been linked to protein misfolding (*22*) and loss of metabolic suppression, leading to enhanced protein secretion (*23*).

In PD, misfolded α-synuclein (αSyn) aggregates in the cytosol and eventually leads to cellular death (*24, 25*). Multiple regions in the nervous system are gradually affected, which results in a plethora of motor and nonmotor symptoms (*26–28*). Synucleinopathy in PD may start in the autonomic system, brainstem, or olfactory bulb; it spreads extracellularly, eventually reaching the mesencephalon and cortical structures (*29*). Thus, both intracellular and extracellular αSyn are targets of disease-modifying treatments, some designed to decrease the cytosolic deposition that leads to neurodegeneration (*30*) and others to prevent its spreading, which is correlated with disease progression (*31*). The failing ubiquitin-proteasome system has been shown to contribute to PD pathology and may constitute an intracellular target (*32*). Autophagy, an intracellular clearing pathway, has been reported to directly affect neurodegeneration

[1]Department of Neurology, University Hospital Zurich (USZ), Frauenklinikstrasse 26, Zurich 8091, Switzerland. [2]University of Zurich (UZH), Neuroscience Center Zurich (ZNZ), Winterthurerstrasse 190, Zurich 8057, Switzerland. [3]ETH Zurich, Neuroscience Center Zurich (ZNZ), Winterthurerstrasse 190, Zurich 8057, Switzerland. [4]ETH Zurich, Laboratory of Physical Chemistry, Department of Chemistry and Applied Biosciences, Vladimir-Prelog-Weg 2, Zurich 8093, Switzerland. [5]Center of Competence Sleep and Health Zurich, University of Zurich, Frauenklinikstrasse 26, Zurich 8091, Switzerland.
*Corresponding author. Email: daniela.noain@usz.ch
†These authors contributed equally to this work.

and αSyn quantity (*33*, *34*). In addition, αSyn cell-to-cell propagation through exosome release (*31*) may allow extracellular αSyn to be eliminated by glymphatic clearance (*35*–*37*). Glymphatic clearance might be compromised in PD by the cumulative effect of sleep-wake disturbances, toxic effects of aggregated αSyn, and the impact of dopaminergic degeneration on aquaporin-4 (AQP4) function (*38*). Furthermore, because glymphatic clearance is highest during sleep and sleep-like brain activity (*16*), altered sleep and circadian rhythms might limit opportunities for the glymphatic system to operate (*38*).

In summary, sleep-wake disturbances are highly prevalent in patients with PD (*28*), and recent evidence has shown that SD produces increased αSyn and phosphorylated αSyn in CSF (*39*, *40*). However, in contrast to AD, no preclinical study has explored SE as a potential disease-modifying intervention for PD. Therefore, in this study, we tested whether modulating SWS affects αSyn burden in two synucleinopathy-expressing transgenic mouse models. In addition, to explore putative target mechanisms underlying a role of SWS as neuroprotective agent, we explored a range of markers associated with glymphatic clearance and protein degradation. To broaden our view of the potential mechanisms affected by sleep modulation, we compared the proteomes of sleep-modulated mice and compared protein enrichment in functional clusters linked to proteostasis.

RESULTS

Increased arousal, reduced sleep efficiency, and slowing of REM theta oscillatory activity in young VMAT2 LO mice

Human PD is associated with a variety of sleep-wake disturbances, including multifactorial insomnia, excessive daytime sleepiness, and parasomnias (*41*, *42*), some of which may manifest in premotor stages of PD (*43*). To determine the characteristics of natural sleep-wake patterns in early-stage vesicular monoamine transporter 2 (VMAT2)–deficient (LO) mice, we compared electroencephalography/electromyography (EEG/EMG)–determined sleep-wake proportions in unmedicated mutant mice and wild-type (WT) siblings at 5 months of age (fig. S1, A to C). We observed increased wakefulness (WAKE, *$P < 0.05$), reduced non-REM sleep (NREM, *$P < 0.05$), and REM sleep (***$P < 0.001$) in LO mice compared to WT (fig. S1D). The changes were most salient at the beginning of the dark period (WAKE: 14 hours **$P < 0.01$, 16 hours ***$P < 0.001$; NREM: 16 hours **$P < 0.01$; REM: 16 hours *$P < 0.05$). Overall, there were significant differences between the genotypes in the dark phase (*$P < 0.05$) but not in the light one. The cumulative analysis confirmed that LO mice spent more time awake than WT mice (dark period *$P < 0.05$; fig. S1D, top), and less time in NREM (dark period *$P < 0.05$; fig. S1D, middle) and REM sleep (dark period *$P < 0.05$; fig. S1D, bottom). In addition, we observed decreased sleep efficiency in mutants compared to WT littermates over 24 hours (**$P < 0.01$; fig. S1E, top) and in the dark period (*$P < 0.05$; fig. S1E, middle), whereas no changes were noted in the light period (fig. S1E, bottom).

Conversely, slowing of oscillatory activity, especially in the theta band, has been reported to be associated with both aging and neurodegenerative diseases (*44*, *45*). Spectral analyses in WAKE, NREM, and REM sleep in mutants and WT displayed no significant changes in the spectrograms corresponding to WAKE (fig. S1F, top) and NREM sleep (fig. S1F, middle), but we found significant general slowing of theta frequency in REM sleep of LO mice compared to WT (***$P < 0.001$; fig. S1F, bottom). However, total theta power in LO mice compared to WT controls was unchanged ($P > 0.05$; fig. S1G). In terms of sleep stability, we observed no differences in the fragmentation index of any vigilance state in LO mice compared to controls (fig. S1H).

Behavioral and pharmacological SWS manipulations affect slow-wave energy

Sodium oxybate, a salt of central nervous system depressant γ-hydroxybutyrate, is primarily used to reduce excessive daytime sleepiness and cataplexy in narcolepsy (*46*). The drug effects are predominantly mediated by activation of γ-aminobutyric acid type B receptors. Both sodium oxybate administration and SD exert effects on slow-wave activity (SWA) during SWS (*47*, *48*). However, therapeutic dosing varies greatly across literature and species, and preclinical oral administration has been poorly explored. Thus, we first quantified changes in both spectral power and time spent in NREM sleep (Fig. 1, A to D) in the first 2 hours after two oral administrations (light and dark period), when changes in oscillatory activity induced by the drug are most prominent, upon administration of saline vehicle or sodium oxybate (100, 200, or 400 mg/kg; Xyrem, UCB Pharma) in young WT mice ($n = 4$). Guided by the aim of exploring the neuroprotective effects of increasing depth of sleep rather than its duration, for our long-term interventions, we chose 200 mg/kg as optimal dosage given its SWA enhancement effect (P values ranging from *$P < 0.05$ to ****$P < 0.0001$ in different frequency bind within the delta range) in both light and dark periods (Fig. 1, A and B) without inducing changes ($P > 0.05$) in NREM sleep proportion (Fig. 1, C and D). We then explored the effect of the selected dose of sodium oxybate (200 mg/kg) on WAKE and REM sleep proportions and spectral patterns (fig. S2). We observed no changes in WAKE and REM proportions in either dark or light period with sodium oxybate (200 mg/kg) compared to vehicle ($P > 0.05$; fig. S2, A to D). As for WAKE and REM spectral patterns, we detected minimal alterations in WAKE, with sodium oxybate slightly increasing power in the delta band in both dark and light periods (WAKE dark $P > 0.05$; WAKE light $P > 0.05$; fig. S2, E and F). Sodium oxybate additionally triggered a discrete power increase around 13.5 Hz (low beta range) in REM sleep only in the light period (REM dark $P > 0.05$; REM light $P = 0.002$; fig. S2, G and H).

To assess the quantitative effect of SWS manipulation with SE using sodium oxybate (200 mg/kg, orally) and with SD using the platform-over-water method (*5*) for 16 hours/day on sleep depth and stability, we acquired EEG/EMG recordings from aged mice ($n = 19$) at baseline (24 hours) and under three experimental conditions (24 hours): placebo (P), $n = 5$; SE, $n = 7$; and SD, $n = 7$ (Fig. 1E). Because chronic EEG implantation can alter glymphatic function in mice (*49*) and because aged transgenic mice did not tolerate EEG/EMG implantation well, an additional cohort of WT mice was assessed. We determined cumulated SWA, otherwise called slow-wave energy (SWE; integral of EEG power density in delta frequency band range) (*50*), in the 12-hour light period and the fragmentation index as indicators of sleep depth and stability, respectively. During the treatment day, SE with sodium oxybate (200 mg/kg) increased SWE during SWS (mean ratio: 691.3, SEM: 264.5) relative to baseline (*$P < 0.05$; Fig. 1F), whereas SD reduced SWE during SWS (mean ratio: −419.6, SEM: 108.8) relative to baseline (*$P < 0.05$; Fig. 1F). In addition, SD produced increased SWS fragmentation
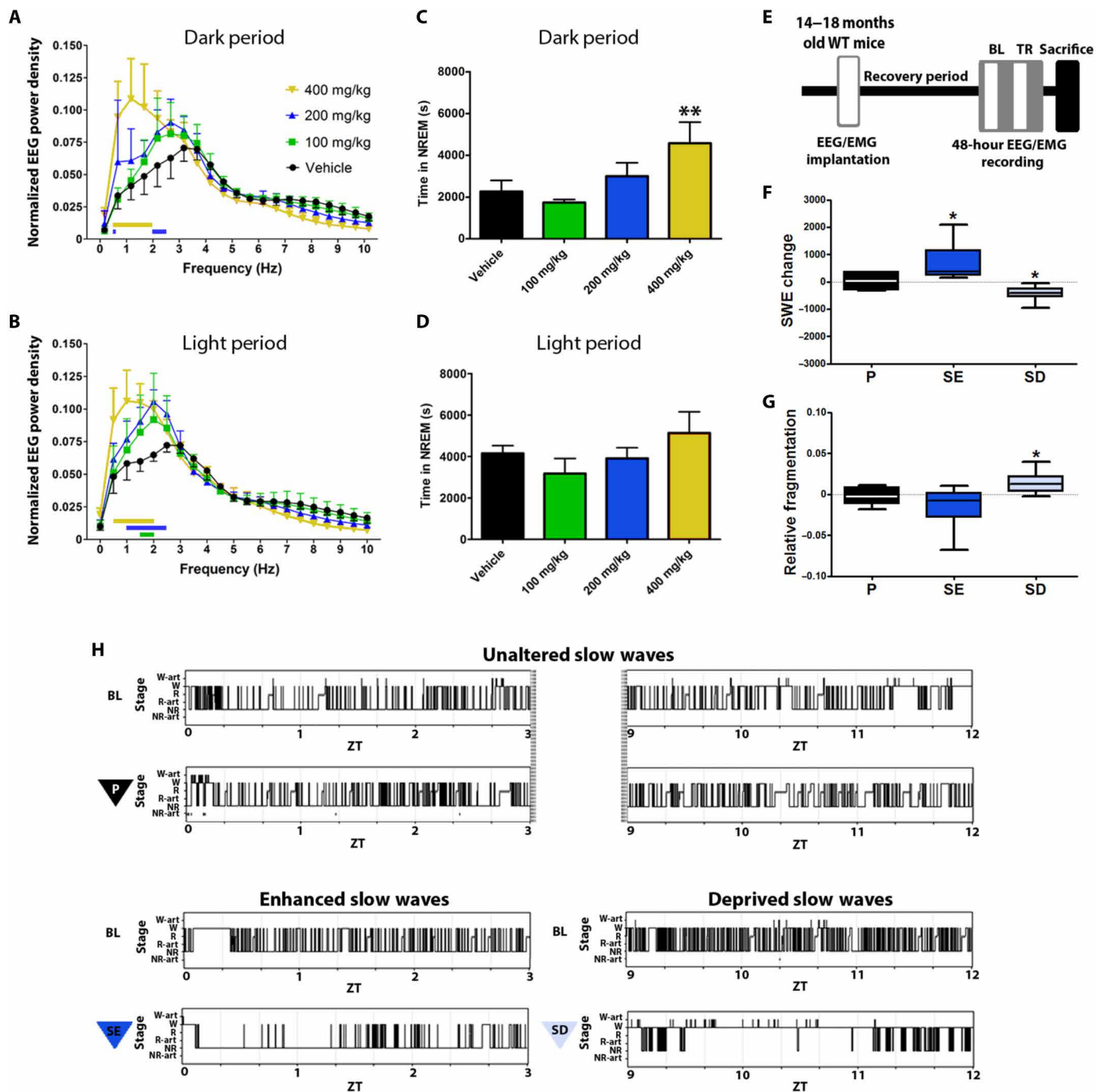
Fig. 1. Changes in SWE and fragmentation index associated with slow-wave deprivation or enhancement with sodium oxybate (200 mg/kg). Dose-response curve for spectral density (**A** and **B**) and time (**C** and **D**) in NREM sleep 2 hours after oral administration of saline vehicle or sodium oxybate (100, 200, or 400 mg/kg) in 3-month-old WT mice ($n = 4$) during the dark (A and C) and light (B and D) periods. Effects on delta power: repeated-measures ANOVA and Dunnett's comparisons for 100 mg/kg (green), 200 mg/kg (blue), and 400 mg/kg (yellow) orally administered sodium oxybate. Significant differences [two-way ANOVA, dark period: frequency*treatment $F_{60,252} = 4.093$, ****$P < 0.0001$ and light period: frequency*treatment $F_{60,252} = 3.689$, ****$P < 0.0001$; dark and light Bonferroni multiple comparisons test P values ranging from *$P < 0.05$ to ****$P < 0.0001$] in specific frequency bins within the low delta range are represented by bin-locked color horizontal bars for each dose compared to vehicle. Effects on NREM sleep time: repeated-measures ANOVA, dark period, vehicle versus 400 mg/kg, **$P < 0.01$. We chose 200 mg/kg as dose for the modulation experiments. (**E**) Forty-eight hours of EEG/EMG recordings from aged WT animals were collected at baseline and under three treatment regimens [P, $n = 7$; SE, $n = 7$; SD, $n = 7$ (P final $n = 5$; two mice were excluded because of poor signal quality)]. (**F**) Effect of slow-wave modulation on SWE in the light period (SE relative to baseline: Wilcoxon signed-rank test, *$P < 0.05$; SD relative to baseline: Wilcoxon signed-rank test, *$P < 0.05$). (**G**) SWS fragmentation index in the light period after SD (Wilcoxon signed-rank test, SD relative to baseline: *$P < 0.05$). (**H**) Representative hypnograms (ZT 1 to 3: depicting effect of sodium oxybate administration; ZT 9 to 12: depicting effect of SD) of WT mice at baseline and under P, SE, and SD treatment. W, wakefulness; W-art, artifact in wakefulness; NR or NREM, nonrapid eye movement sleep; NR-art, artifact in NREM; R, rapid eye movement sleep; R-art, artifact in REM; WT, wild-type; EEG/EMG, electroencephalogram/electromyogram; SWE, slow-wave energy; P, placebo; SE, slow-wave enhancement; SD, slow-wave deprivation; BL, baseline; ZT, Zeitgeber..

(mean: 0.0145, SEM: 0.005, *$P < 0.05$; Fig. 1G) compared to baseline, whereas SE did not affect SWS continuity ($P > 0.05$; Fig. 1G). Exploring hypnograms of placebo-, SE-, and SD-treated mice at baseline and treatment day in relevant time windows revealed that whereas hypnograms in the placebo group remained unaltered (Fig. 1H, top), SE treatment enhanced slow waves and thus the amount of scored NREM sleep during the treatment day compared to baseline (Fig. 1H, left bottom). SD intervention exerted the opposite effect (Fig. 1H, right bottom).

Reduced prefrontocortical αSyn neuropathology in SWS-enhanced aged VMAT2 LO mice and opposite effect in sleep-deprived mice

SE has been reported to decrease protein burden in some neurological diseases (5, 47); however, to the best of our knowledge, the effect has never been explored in PD models. Thus, we assessed the effect of 4 months of sleep-modulating interventions on αSyn burden in LO mice. Although increased αSyn burden has been reported before in LO mice (51, 52), a detailed anatomical description of the neuropathological pattern is not available. Therefore, to determine the region of interest for testing the impact of sleep modulations on αSyn burden in this model, we first performed a total αSyn (Syn^{total}) immunostaining analysis in sagittal hemibrain sections from aged LO mice and controls. Through qualitative evaluation of signal pattern and intensity (fig. S3), we observed that the most salient differences between WT (fig. S3A) and LO (fig. S3B) brains were restricted to the prefrontal cortex (PFCx) followed by milder differences in other nuclei such as the pontine nucleus (Pn), substantia nigra, striatum, and hippocampus. To confirm this observation quantitatively, we cut the complementary hemibrain coronally and again stained for Syn^{total}, now followed by blinded stereological cell counting in the PFCx and Pn, the latter as proxy of all other structures more mildly affected. The results confirmed that PFCx presented significantly higher Syn^{total} immunoreactive cell counts in LO brains than in WT ones (*$P < 0.05$; fig. S4, A and C), but cell counts in the Pn were not significantly different between genotypes ($P > 0.05$; fig. S4, B and D).

After 4 months of treatments (Fig. 2A), we performed a broad neuropathological study of the region of interest [PFCx: from +3.05 to +1.97 mm (53); Fig. 2B] in coronal hemibrain tissue obtained from sleep-modulated (SE and SD) and placebo-treated (P) LO and WT mice sacrificed at 18 months of age. Stainings included thioflavin S, mild proteinase K digestion followed by total αSyn (PK + Syn^{total}), nitrated αSyn (Syn$^{Nitrate-Tyr125/133}$), and phosphorylated αSyn (Syn$^{Phospho-S129}$) (table S1), which are all widely recognized as markers of synucleinopathy in humans, animals, and cultured cells (54–58). Thioflavin S staining yielded inconclusive results in signal intensity and distribution between the treatment groups (fig. S5). In contrast, the visual inspection of the three specific immunostainings (Fig. 2, C to E) presented more obvious differences between genotypes and treatments, with LO P mice displaying more densely stained sections of PFCx than WT P mice, and with SE and SD treatments decreasing and increasing signal intensity, respectively. To validate these observations quantitatively, we followed Syn^{S129} staining with examiner-blinded stereological counting (WT P $n = 6$, WT SE $n = 7$, WT SD $n = 6$, LO P $n = 7$, LO SE $n = 6$, LO SD $n = 6$, with seven to nine sections per mouse). We found significantly higher stereological counts of Syn^{S129} immunoreactive (Syn^{S129}-IR) cells in the cortex of LO P compared to WT P (**$P < 0.01$; Fig. 2F). LO SE showed lower Syn^{S129} immunoreactivity than LO P (**$P < 0.01$; Fig. 2F), whereas LO SD revealed higher cortical Syn^{S129} cell counts than the LO P group (***$P < 0.001$; Fig. 2F).

To confirm these histological results, we performed a series of Western blot analyses of PFCx tissue samples from the sleep-modulated WT and LO mice (Fig. 2G and fig. S6). These examinations showed a higher amount of Syn^{S129} in LO P than in WT P mice and lower Syn^{S129} amounts in LO SE mice (Fig. 2G). However, we found a low amount of Syn^{S129} in the LO SD group. Because SD has been associated with increased protein misfolding and aggregation (22), we conceived that SD treatments in LO mice could have disproportionally increased αSyn aggregation, which would not be ideally identified by conventional Western blot that mainly detects soluble proteins (59). We thus performed a soluble/insoluble fraction separation of WT and LO PFCx samples and ran LB509 Western blot on the insoluble fraction to determine the relative amount of aggregated αSyn in each treatment group (Fig. 2H). As expected, we observed very low, although detectable, amounts of insoluble αSyn in the WT P and WT SE groups, whereas WT SD brains presented a higher insoluble αSyn load. In LO mice, we confirmed higher aggregated/insoluble αSyn content upon SD as compared to LO P mice, whereas the LO SE samples presented with the lowest quantity of aggregated/insoluble αSyn of all three treatments in this genotype.

Our results show detectable amounts of αSyn neuropathology in 18-month-old WT brains (Fig. 2, C to H). This supports the notion of age being a strong contributing factor to naturally occurring pathological αSyn deposition in otherwise healthy brains (60). In line with this notion, we found that 3-month-old WT brains did not present any detectable Syn^{S129}-IR (fig. S7A), but brains from 3-month-old LO mice already showed strong signs of pathology (fig. S7B), in opposition to earlier studies reporting an onset of αSyn pathology only at around 18 months of age in this line (51, 52).

In addition, we explored whether slow-wave modulation treatments had a symptomatic effect at a behavioral level in PD mice. At baseline, 14-month-old LO mice presented significantly lower locomotor activity (*$P < 0.05$; fig. S8A) and higher time of immobility (***$P < 0.001$; fig. S8B) than WT controls. At treatment end point, we determined that slow-wave modulations did not have a major effect on LO mice, still performing significantly worse than WT mice either on locomotion (***$P < 0.001$; fig. S8C) or on their time of immobility (***$P < 0.001$; fig. S8D). The end point versus baseline analysis of locomotor performance (fig. S8E) and immobility rates (fig. S8F) also showed that, regardless of the treatment group, LO mice did not significantly deteriorate or improve their performance compared to WT controls.

Reduced amounts of aggregated human αSyn in the A53T transgenic mice

Synucleinopathy in LO mice is likely an emergent property of a myriad of conditions propitiated by the transporter gene mutation and, therefore, of unclear origin and characteristics (51). These key uncertainties warranted confirmation of the effect of sleep modulation treatment on αSyn burden in an independent model of well-characterized and understood synucleinopathy. We assayed a 4-month SE protocol with sodium oxybate in 5.5-month-old male and female A53T mice, an established transgenic mouse line expressing and burdened by human αSyn carrying a mutation associated with familial PD (61), and strain-, age-, and sex-matched WT controls (Fig. 3A). We observed no onset of marked pathological
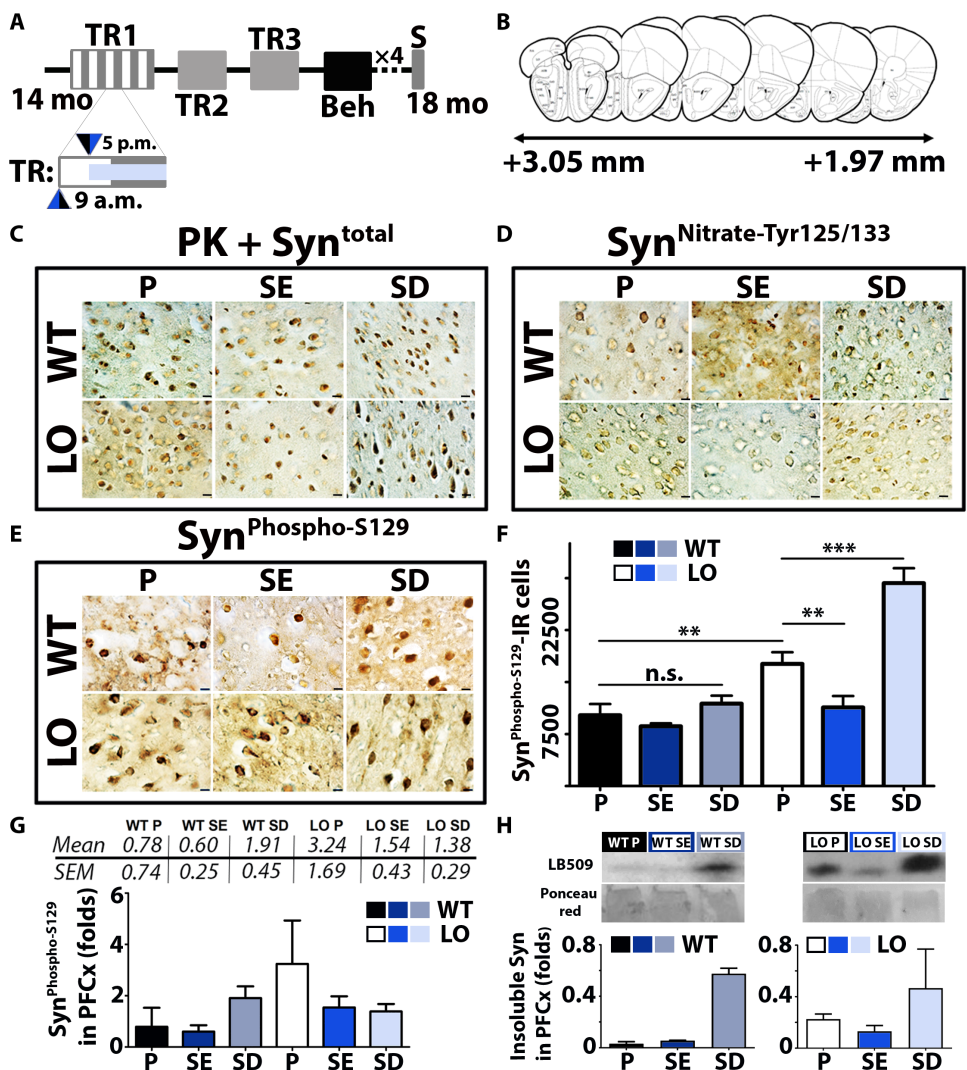
Fig. 2. Changes in prefrontocortical αSyn neuropathology after long-term slow-wave modulation in VMAT2 LO mice. (**A**) Experimental timeline: We subjected VMAT2 LO and WT mice to a slow-wave modulation paradigm consisting of slow-wave enhancement (blue triangles: twice a day administration of 200 mg/kg sodium oxybate, orally) and deprivation (light blue rectangle: twice a day administration of placebo, black triangles, orally + 16 hours/day platform over water) for 4 months, beginning at 14 months of age. We treated WT placebo (WT P, $n = 7$), WT slow wave–enhanced (WT SE, $n = 7$), WT sleep-deprived (WT SD, $n = 7$), LO placebo (LO P, $n = 7$), LO slow wave–enhanced (LO SE, $n = 7$), and LO sleep-deprived (LO SD, $n = 7$) groups for 5 days per week, 3 weeks per month, for 4 months, until 18 months of age. We dedicated the fourth week of each round to behavioral testing under no treatment. (**B**) Schematic representation of some of the coronal sections included in stereological analysis given the region of interest selected earlier. Representative images (63×) of prefrontocortical sections of the treatment groups and genotypes immunostained for pathological αSyn with (**C**) proteinase K + anti–total αSyn (PK + Syn^{total}) (1:1000; no. 2642, Cell Signaling Technology), (**D**) anti–nitrated αSyn (Syn$^{Nitrate-Tyr125/133}$) (1:400; no. MA5-16142, Thermo Fisher Scientific), and (**E**) anti–phosphorylated αSyn (Syn$^{Phospho-S129}$) antibodies (1:1000; no. AB59264, Abcam). (**F**) Stereological quantification of Syn^{S129}-IR cell counts in WT P, WT SE, WT SD, LO P, LO SE, and LO SD mice [factorial ANOVA, $F_{2,32} = 11.790$, $P = 0.00015$; post hoc comparisons of Fisher's least significant difference (LSD): LO P versus WT P **$P < 0.01$; LO P versus LO SE **$P < 0.01$; LO P versus LO SD ***$P < 0.001$]. No significant (n.s.) changes among the WT groups ($P > 0.05$). (**G**) Western blot analysis of Syn^{S129} amount (1:500; no. AB59264, Abcam), normalized to glyceraldehyde-3-phosphate dehydrogenase (GAPDH; 1:10,000, MA5-15738, Thermo Fisher Scientific) as loading control in sleep-modulated WT and LO subjects ($n = 2$ per group). (**H**) Western blot representative images and quantification of αSyn in the insoluble fraction detected with LB509 (1:1000; ab27766, Abcam) in sleep-modulated WT ($n = 2$ per group) and LO ($n = 3$ per group) mice. Bands from the insoluble fraction were normalized to Ponceau red used as loading control. LO, vesicular monoamine transporter 2–deficient; WT, wild-type; Syn$^{Phospho-S129}$ or Syn^{S129}, serine-129 phosphorylated αSyn; Syn^{S129}-IR, Syn^{S129} immunoreactive cells; Syn$^{Nitrate-Tyr125/133}$ or Syn$^{125/133}$, nitrated αSyn; Syn^{total}, total αSyn; PK, proteinase K; TR, treatment. Scale bars, 10 μm.

phenotypes such as impaired weight progression, paralysis, or lack of grooming at any time point of the study until the time of sacrifice at 9.5 months of age in either male or female mice of any treatment group (fig. S9A).

Biochemical and histopathological results obtained from brain samples of male A53T mice broadly confirmed our previous observation in LO mice: SE with sodium oxybate markedly reduced the amounts of high–molecular weight (HMW or aggregated) αSyn in A53T midbrains compared to placebo-treated A53T mice (>70% overall reduction, ***$P = 0.0003$; Fig. 3, B and C). This reduction in HMW content in A53T SE rendered it indistinguishable from that one of WT P mice ($P > 0.05$; Fig. 3, B and C). Reduced pathological protein burden was also shown by Syn^{303} immunohistochemistry on brain sections from male A53T SE mice when compared to placebo-treated A53T mice (Fig. 3D). However, we did not observe a similarly strong beneficial effect of SE in female A53T brains compared to A53T P females (only ~30% overall reduction, $P = 0.0014$; fig. S9, B and C). This result was also evident in Syn^{303} immunohistochemistry examinations (fig. S9D).

Driven by the observation of dissimilar SE benefit in A53T males and females, we explored whether gender differences exist in the response to oral administration of sodium oxybate. We recorded a drug-naïve 24-hour baseline (BL) followed by a 24-hour SE period with twice daily (light onset and 8 hours later, morning and evening doses) administration of sodium oxybate (300 mg/kg, orally) in male ($n = 4$) and female ($n = 4$) WT mice. We found an attenuated effect of sodium oxybate (TR) on mean delta power relative to baseline (TR/BL) after the morning administration [Zeitgeber (ZT) 1 to 6, *$P = 0.04$; fig. S9E] in female mice compared to males, whereas both sexes presented a similar cumulative response to the evening dose (ZT 8 to 13, $P > 0.05$; fig. S9E).

Slow-wave enhancement associated with elevated AQP4 recruitment to perivascular sites in aged VMAT2 LO mice brains

The glymphatic pathway, through its key regulator AQP4 (62), has previously been linked to clearance of extracellular
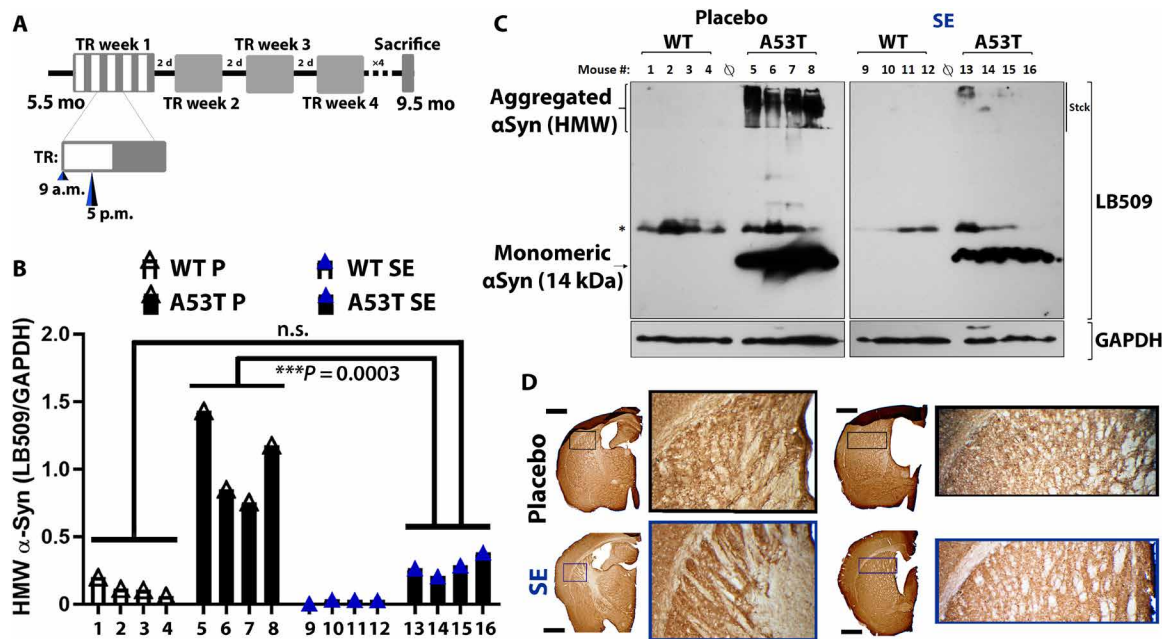
Morawska et al., Sci. Transl. Med. **13**, eabe7099 (2021)   8 December 2021

5 of 13

Fig. 3. Reduced human αSyn burden in sodium oxybate–treated male A53T mice compared to mice administered with placebo. (**A**) Experimental timeline for A53T animals and their WT controls: We pharmacologically treated A53T mice (n = 16, 1 male:1 female) and WT controls (n = 16, 1 male:1 female) with either placebo [P; black triangles; A53T males n = 4, WT males n = 4 (A53T females n = 4, WT females n = 4 are shown in fig. S9)] or slow wave–enhancing drug sodium oxybate [SE; blue triangles; twice a day administration (200 mg/kg, orally) at lights ON and 8 hours later; A53T males n = 4, WT males n = 4 (A53T females n = 4, WT females n = 4 are shown in fig. S9)] 5 days per week for 16 weeks. (**B**) Quantification of high–molecular weight (HMW) α-Syn assessed by LB509 Western blot in male A53T mice subjected to SE compared to male A53T placebo-treated controls [two-way ANOVA, $F_{3,9}$ = 35.66, Tukey's multiple comparisons A53T P*A53T SE, ***P = 0.0003, WT P*A53T SE, P > 0.05]. (**C**) Top: Representative LB509 Western blot image from WT P (lanes 1 to 4), A53T P (lanes 5 to 8), WT SE (lanes 9 to 12), and A53T SE (lanes 13 to 16). Bottom: GAPDH blots used as loading controls. *, unspecific bands. (**D**) Specific anti-Syn[303] [1:1000; catalog no. 824301, BioLegend (previously Covance MMS-5085)] 3,3'-Diaminobenzidine (DAB)-immunohistochemistry on A53T P and A53T SE 40-μm free-floating brain sections. TR, treatment; mo, months old; GAPDH, glyceraldehyde 3-phosphate dehydrogenase, Stck, stocking; ∅, empty lane. Scale bars, 1 mm.

metabolites during sleep (16). Perivascular recruitment of AQP4 appeared altered in autopsy brains of patients with AD (63), indicating that localization of the protein may play an important role in neurodegeneration. Thus, we explored whether SE and SD change perivascular recruitment of AQP4 via immunofluorescence studies on PFCx samples from sleep-modulated WT and LO mice (Fig. 4). Semiquantitative analysis of double immunofluorescence studies in hemicoronal PFCx sections using antibodies against glial acidic fibrillary protein (GFAP; pink signal; Fig. 4A), a marker of astrocytes, and AQP4 (turquoise signal; Fig. 4A) showed a significant increase in the ratio of perivascular/parenchyma AQP4 signal in LO SE brains compared to all other groups (P values ranging from *P < 0.05 to **P < 0.01; Fig. 4B). Protein expression mass spectrometry's data indicated no changes in overall AQP4 expression in the PFCx, as shown by similar AQP4 to total protein content ratios among all genotypes and treatment groups (P > 0.05; Fig. 4C).

To explore alternative degradation mechanisms by which αSyn neuropathology burden could be affected (32–34), we also assayed double immunofluorescence studies using antibodies against Syn[S129] (pink signal, fig. S10, A and B) and ubiquitin, a tag for the ubiquitin-proteasome degradation pathway (turquoise signal, fig. S10A), or light-chain microtubule-associated protein 3B (LC3B), a tag for endosome-lysosome degradation (turquoise signal, fig. S10B). Visual assessments of confocal microscopy images showed similar colocalization (dark violet, fig. S10, A and B) pattern in the PFCx among treatment groups, which suggests comparable proteasomal

and autophagic degradation in all groups. Moreover, expression of these individual proteins was similar among all groups when assessed by mass spectrometry quantification (fig. S10, C and D).

Slow-wave enhancement associated with up-regulated proteostatic pathways

Although quantification of single specific target proteins possibly related to sleep-induced neuroprotection provides valuable insights, the effects of sleep on cell and protein homeostasis may well be broad and warrant a more comprehensive examination. Thus, to determine potentially wider downstream effects of sleep modulation in healthy (WT) and diseased (LO) brains, we launched mass spectrometry determinations for bulk protein quantification in WT P (n = 6), WT SE (n = 6), WT SD (n = 6), LO P (n = 6), LO SE (n = 5), and LO SD (n = 6) 30-μm-thick hemicoronal PFCx sections. For the proteins found to be significantly modulated (P < 0.05; fig. S11A), we ran functional clustering and enrichment score analyses (DAVID web tool) that identified 150 functional clusters. We selected 10 clusters particularly relevant for protein-triggered neurodegenerative processes (see table S2) because of their involvement in either protein or cellular homeostasis (Fig. 5A). For these 10 clusters, we created heatmaps of all six groups (fig. S11, B to K) or of WT and LO groups separately (Fig. 5, B to K). Although each functional cluster analyzed presents an individual pattern of up- and/or down-regulation associated with sleep modulation treatments, the overall results indicate that SE in LO mice induces up-regulation
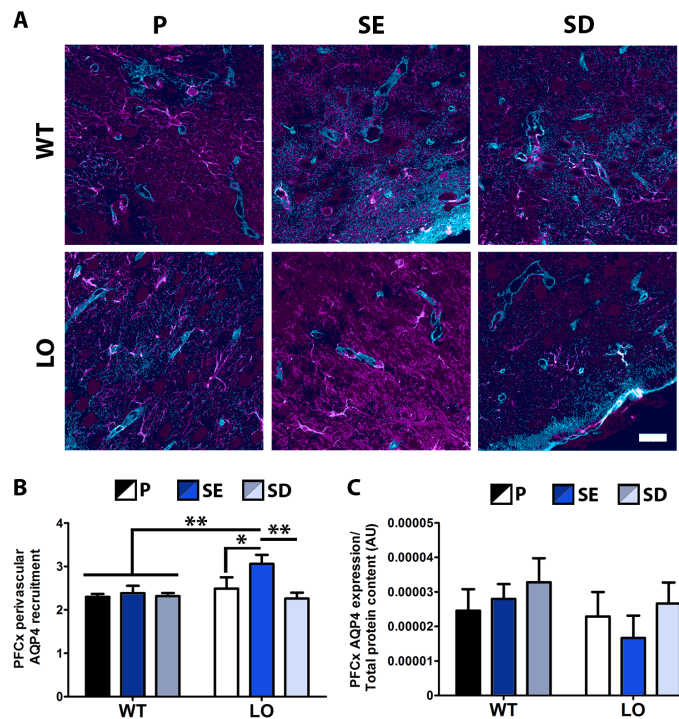
Fig. 4. Increased perivascular recruitment of AQP4 in association with SE in VMAT2 LO mice. (**A**) Immunofluorescence colocalization studies between GFAP (pink signal, 1:500; no. AB5541, Millipore) and AQP4 (turquoise signal, 1:800; no. AB3594 Millipore) in PFCx of VMAT2 LO and WT sleep-modulated mice. (**B**) Semi-quantitative analysis of perivascular versus parenchymal AQP4 signal in all groups [factorial ANOVA: $F_{2,30} = 3.5854$, treatment effect *$P < 0.05$, Fisher's LSD post hoc comparisons: LO SE versus WT P, **$P < 0.01$; LO SE versus WT SE, **$P < 0.01$; LO SE versus WT SD, **$P < 0.01$; LO SE versus LO P, *$P < 0.05$; LO SE versus LO SD, **$P < 0.01$]. (**C**) AQP4 protein expression in relation to total protein content in all groups as assessed by mass spectrometry ($P > 0.05$). Scale bar, 20 μm for all pictures. AU, arbitrary units.

of neuroprotective pathways, whereas SD down-regulates them (Fig. 5, B to K, right). SD promoted a change in these clusters in a similar direction in WT mice, but we observed mild down-regulation caused by SE in this genotype group (Fig. 5, B to K, left).
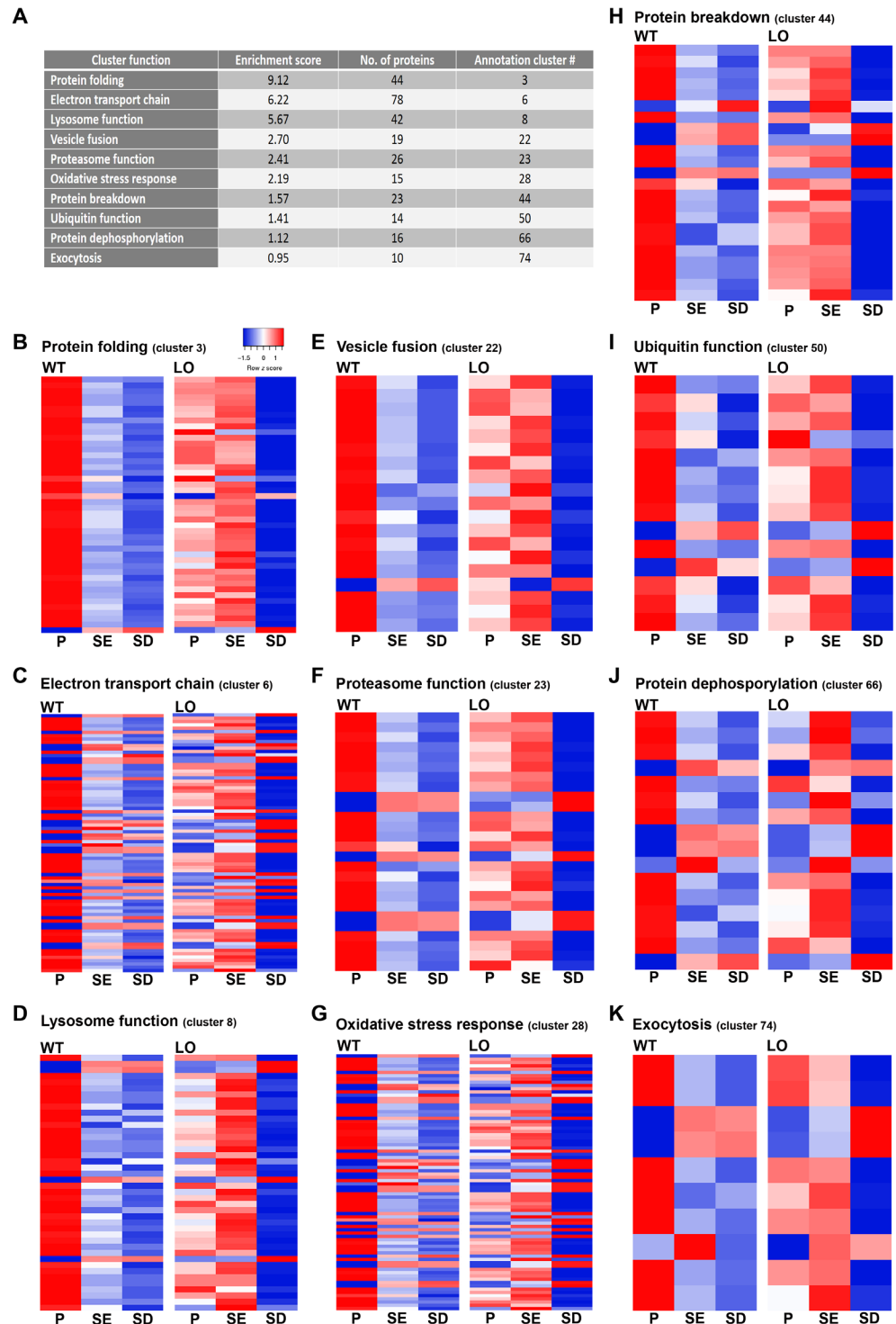
DISCUSSION

This study provides evidence of a beneficial effect of enhanced SWS on neuropathological status in two murine models of synucleinopathy analogous to PD in humans. VMAT2-deficient mice (51, 52, 64) suffer from early sleep-wake and motor disturbances and thus partially resemble patients with PD. VMAT2-deficient mice that underwent long-term SWS enhancement had reduced pathological αSyn burden in their brains, whereas synucleinopathy worsened in chronically sleep-deprived mice. The beneficial effect of SWS enhancement on neuropathology was corroborated in a widely validated synucleinopathy model, the A53T mouse (61). The alleviated αSyn burden promoted by enhanced sleep in VMAT2 mice was accompanied by up-regulation of multiple protein and cell homeostasis pathways. However, long-term slow-wave modulation at advanced age did not have a symptomatic effect on motor ability or progression in VMAT2 mice.

Sleep-wake disturbances are present in many neurological diseases. In PD, some appear in the prodromal stage (65), whereas others are the consequence of disease progression and symptomatic treatments (13). To assess possible early sleep-wake disturbances in the VMAT2-deficient mice, we performed EEG/EMG recordings at 5 months of age. Although sleep-wake disturbances in LO mice start early in the course of disease as they do in patients with PD, the characteristics differ between species. In human PD, REM sleep behavior disorder often precedes motor symptoms. Early sleep-wake disturbances in LO mice, by contrast, included increased wakefulness in the first hours of the active phase at the expense of both NREM and REM sleep, leading to decreased sleep efficiency, and a prominent slowing of oscillatory activity in REM sleep. We observed no changes in theta power or sleep stability. Insomnia and loss of deep sleep can manifest early in patients with PD but are present mostly in advanced stages of the disease (1–3, 66). The slowing in theta frequencies observed in the mutant mice is a well-described phenomenon present in other neurodegeneration models (67, 68) and in patients with PD (44) and may reflect ongoing neurodegenerative processes (69). Moreover, oscillatory activity in REM sleep has been linked to vascular activity (19), suggesting a potential role for these oscillations in glymphatic function (20). In addition, the shift in the pattern of wakefulness in young mice could impair glymphatic efficiency because the system has recently been reported to be under circadian control (70).

Recent evidence suggests that poor sleep can aggravate protein deposition and the neurodegenerative process (71–73). SE and SD over 4 months in LO mice started around the onset of protein deposition previously described (51) and affected αSyn neuropathology; this was qualitatively assessed by markers such as proteinase K–resistant and nitrated αSyn deposits and quantitatively corroborated by altered prefrontocortical Syn[S129]-IR cell counts. LO mice treated with placebo presented higher Syn[S129]-IR cell counts than WT mice in the same treatment group, indicating elevated synucleinopathy and confirming the suitability of both the selected region of interest and Syn[S129] marker as a proxy for neuropathological status. The main finding here is the reduced number of Syn[S129]-IR cells in SE-treated LO mice compared to placebo-treated mutants, a finding corroborated in an independent synucleinopathy line, A53T mice. In contrast, in LO mice subjected to SD, Syn[S129] burden was further increased compared to controls. Confirmatory Western blot results mirrored these histological results, with both LO P presenting higher neuropathological markers than WT P and LO SE showing lower amounts than LO P counterparts. Furthermore, SD was associated with an overall increased quantity of insoluble αSyn relative to placebo in both WT and LO mice, in agreement with reports on protein misfolding and, hence, higher quantities of insoluble aggregates being associated with SD (22).

SE also had a strong (~70%) beneficial effect on αSyn burden in male A53T mice, quantitatively determined via Western blot with LB509 antibody and qualitatively confirmed by Syn303 immunostaining. We found a more modest effect (~30%) of sodium oxybate treatment on αSyn pathology in female A53T mice. Although gender differences in neurodegeneration and inflammation have recently been explored in A53T mice (74), further exploration on sexually dimorphic αSyn neuropathology is warranted. On the other hand, despite increasing numbers of drugs presenting sexually dimorphic responses (http://womensbrainproject.com/), such responses have not yet been explored for sodium oxybate. We provide

Morawska *et al.*, *Sci. Transl. Med.* **13**, eabe7099 (2021)   8 December 2021

7 of 13

Fig. 5. Effect of sleep modulation treatments on protein expression within homeostasis-related functional clusters in WT and VMAT2 LO mice. (**A**) Table of 10 selected functional clusters including their assigned name, enrichment score according to DAVID web tool, number of proteins in the cluster, and annotation number within the general cluster list (table S2, in order of appearance in the heatmaps). We compared the effect of treatments per genotype on protein folding (**B**), electron transport chain (**C**), lysosome function (**D**), vesicle fusion (**E**), proteasome function (**F**), oxidative stress response (**G**), protein breakdown (**H**), ubiquitin function (**I**), protein dephosphorylation (**J**), and exocytosis (**K**) clusters. LO brains in right panels and WT brains in left panels.

A

Cluster function	Enrichment score	No. of proteins	Annotation cluster #
Protein folding	9.12	44	3
Electron transport chain	6.22	78	6
Lysosome function	5.67	42	8
Vesicle fusion	2.70	19	22
Proteasome function	2.41	26	23
Oxidative stress response	2.19	15	28
Protein breakdown	1.57	23	44
Ubiquitin function	1.41	14	50
Protein dephosphorylation	1.12	16	66
Exocytosis	0.95	10	74

B Protein folding (cluster 3)

C Electron transport chain (cluster 6)

D Lysosome function (cluster 8)

E Vesicle fusion (cluster 22)

F Proteasome function (cluster 23)

G Oxidative stress response (cluster 28)

H Protein breakdown (cluster 44)

I Ubiquitin function (cluster 50)

J Protein dephosporylation (cluster 66)

K Exocytosis (cluster 74)

evidence suggesting a discrepancy in the EEG response to sodium oxybate between genders, with females largely lacking the expected increase in SWA upon morning drug administration. This result allows us to speculate that the "half-response" (namely, response only to evening dose) to the drug observed in females may actually be responsible for the "half-cleared" amounts of HMW αSyn observed in SE A53T female compared to SE A53T male mice. Further investigation of this finding is beyond the scope of the present study but will be explored in future work.

As stated, the exact mechanisms behind alleviated synucleinopathy with deepened sleep, which resembles previous findings in AD mice (5), remain elusive. Emerging theories focus on various aspects of protein processing, degradation, and clearance pathways. The protein release theory proposes that the integrity of SWS is crucial to maintaining low concentrations of extracellular proteins that may otherwise accumulate with toxic effect. It has been shown that neuronal activity, which is most prominent during wakefulness, is associated with exocytosis and amyloid-β release (23), possibly causing increased extracellular amyloid-β concentrations and likely leading to the recently reported augmented concentrations of CSF amyloid-β in humans (8). Moreover, CSF concentrations of other highly relevant neurodegeneration-linked proteins such as tau and αSyn have also been shown to be modulated by sleep intervention (39, 40). Furthermore, recent evidence suggests that sleep might have a neuroprotective function by clearing toxic metabolites that are released to the extracellular space (16). AQP4 has been determined to be a key player in glymphatic function (62) and can be negatively affected by dopaminergic pathology in PD (38). Moreover, diminished perivascular recruitment of AQP4 in human autopsy AD brains was shown to be associated with cognitive

Morawska *et al.*, *Sci. Transl. Med.* **13**, eabe7099 (2021) 8 December 2021

8 of 13

impairment (63), once more highlighting the marked importance of AQP4 perivascular localization and function. We therefore studied AQP4 localization in sleep-modulated LO and WT groups and found its perivascular recruitment augmented in LO SE mice. Increased perivascular recruitment of AQP4 on LO SE brains leads us to speculate that boosting SWS may facilitate glymphatic clearance of extracellular αSyn and therefore reduce its spread and associated pathology.

However, exploring only the glymphatic system and its relation to sleep (16, 18, 75) would limit the identification of downstream mechanisms governing the sleep-mediated neuroprotective effects, which likely involve multiple orchestrated components. Thus, we used neuroproteomics assessments in PFCx samples from WT and LO sleep-modulated mice to more broadly explore the influence of sleep modulation on protein and cellular homeostasis pathways whose impairment has been directly or indirectly linked with neurodegeneration (34, 76–84). In LO mice, slow-wave enhancement emerged as an up-regulator of these homeostatic and neuroprotective processes, including protein folding response, lysosome and proteasome functions, oxidative stress response, electron transport chain, protein breakdown, ubiquitin function, protein dephosphorylation, vesicle fusion, and exocytosis. The same processes were down-regulated in LO sleep-deprived brains, which may explain the impoverished neuropathological status of these mice. Other researchers have already established a link between SD and protein misfolding (22) and phosphorylation (85), which, together with our evidence of reduced HMW (A53T) and insoluble (LO) αSyn amounts in response to SE, supports a direct impact of poor sleep on inefficient protein processing.

In WT brains, the effects of both SE and SD were associated with down-regulation of the same pro-homeostatic pathways. This evidence may suggest that any kind of deviation from the natural slow-wave balance in healthy brains could result in harmful cellular responses, particularly if sustained for long periods. In this regard, SE induced a milder down-regulation than SD in WT brains. These observations fall in line with well-established evidence that both extremes of the natural sleep-wake spectrum, hypersomnia and insomnia, constitute detrimental conditions for human health (86, 87).

On the basis of the evidence presented here, we propose that altered αSyn burden upon long-term SWS modulation (fig. S12A) may be mediated by specific regulation of a myriad of intra- and extracellular processes that regulate proteostasis (fig. S12B, top). In this putative model, intracellular processes, including protein folding response, protein dephosphorylation and breakdown, proteasome and lysosome degradation, and vesicle release, among others, are up-regulated upon slow-wave enhancement (fig. S12B, middle), as suggested by the neuroproteomics results. These mechanisms could lead to decreased amounts of soluble, phosphorylated αSyn, preventing the protein from reaching thresholds at which it can form insoluble aggregates. Moreover, αSyn that is released to the extracellular space could become susceptible to glymphatic clearance, a process that is heightened by augmented recruitment of AQP4 to the astrocytic end feet in the perivascular sites. The increased degradation and clearance may jointly contribute to a reduced pathological protein burden, notably coinciding with the lowered count of αSyn-positive cells. As a result of deprived slow waves (fig. S12B, bottom), by contrast, intracellular proteostatic pathways are down-regulated, resulting in increased accumulation of misfolded phosphorylated αSyn and other pathological species of the protein. This model could elucidate protein dynamics in PD, in which soluble phosphorylated αSyn quantities increase and become insoluble and aggregated over the course of the disease (88), and thus provide a functional link between SWS and symptomatic disease progression (13). However, the exact nature of intra- and extracellular αSyn protein species potentially sensible to the proposed mechanisms' model remains to be carefully determined. For instance, whether exosome- and/or vesicle-associated protein species are handled by the clearance mechanisms in the same manner than soluble proteins, or how the size of exosomes affects its movement through brain tissue, should be put in focus in future research, because it is a critical knowledge gap regarding sleep-mediated protein clearance in the context of neurodegeneration.

Unfortunately, SWS-modulating treatment did not have a major symptomatic effect on motor ability or progression in LO mice. However, we observed that the pathological accumulation of Syn^{S129} starts at least as early as 3 months of age on LO mice, before the onset of motor symptoms, as opposed to 18 months of age, as was reported previously (51, 52). This insight suggests that an SWS-modulating treatment to decelerate the neuropathological process should start at a far earlier stage, at ~3 months old instead of 14 months old, to prevent symptomatic progression. Moreover, the motor symptoms in LO mice were reported to be responsive to levodopa (52), indicating a predominantly dopaminergic origin of the symptoms. However, we did not explore dopaminergic neurodegeneration in these mice, which was reported to reach its peak at 30 months of age (52).

The main limitation of this study is the lack of representative PD models that closely mimic the pathology and symptomatic manifestation of the disease (89). In the present study, the poorly characterized onset of neuropathology in the VMAT2 mouse model limited this model's usefulness for exploring the therapeutic effect of sleep on protein handling and accumulation. However, confirmation of alleviation of αSyn burden with SWS enhancement in a well-established synucleinopathy model (61) corroborated the main outcome of the present study. The frailty of aged VMAT2 mutant mice that disabled EEG/EMG implantations for long-term electrophysiological monitoring of vigilance states during sleep-modulatory interventions constitutes an additional limitation of our approach. We claim, nevertheless, to have obtained the closest possible knowledge on the effect of our sleep interventions on EEG measures of aged mice by evaluating their impact on WT subjects of that age range. On the other hand, further quantitative molecular assessments are needed to indisputably determine the effect of slow-wave modulation on intracellular protein deposits, particularly the interaction between the cellular processes altered downstream of sleep modulations and their direct effects on protein folding and aggregation. Also in this line, our study lacks direct validation of neuroproteomics-identified targets, which shall be explored in careful detail in follow-up research.

Despite the tempting speculations that can be made about the role of slow-wave boosting on the observed synucleinopathy reduction, an intrinsic and non–sleep-mediated drug effect cannot be ruled out in this SE pharmacological paradigm, as was the case in previous studies (5, 16). Moreover, the discrete effect of the administered drug on the low beta band during light period REM sleep shall not be fully ruled out as possible contributor to the observed effect and therefore further explored. On the other hand, although we did not observe stress-related changes in the mice's health status and

changes in stress markers have not previously been reported (5, 90), we cannot fully exclude effects of stress from the current study. However, our observation of a diametrically opposite effect in nonpharmacologically treated SD mice points strongly to a specific role of slow-wave modulation in these results. Moreover, the result that WT female mice only partially increased their SWA in response to the treatment is notably similar to partial effect of SE on pathological αSyn reduction in A53T female mice. Together, these results suggest that a direct relation may exist between SWA increase and the removal of pathological proteins. Nevertheless, future studies should use more specific and sophisticated methods of SWS modulation, for example, auditory slow-wave stimulation. Auditory stimulation in early human trials has shown encouraging effects on memory improvement (91) and even immune function (92), suggesting that selective enhancement of slow waves to modulate sleep depth without changing sleep duration could become a powerful disease-modifying therapeutic tool.

The promising results of this study provide a unique framework that encourages further exploration of the role of SWS in PD pathology. More preclinical and clinical research is needed to (i) find causal links between the proposed underlying pathways and the slow wave–mediated reduction in αSyn burden, (ii) explore the gender differences in effect of SWS modulation on neuropathology, and (iii) fully find the potential of slow-wave modulation as a disease-modifying therapy for PD.

MATERIALS AND METHODS
Study design
The overall study rationale is summarized in fig. S12A. Briefly, the main objective of the study was to assess the potential altering effect of slow-wave modulation on synucleinopathy in the context of murine PD. We executed long-term slow-wave modulation interventions in two mouse models of PD, namely, VMAT2-deficient and A53T mutant mice lines. Characterization of synuclein neuropathology in specific regions of interest via specific immunostaining followed by stereological quantifications was the primary assessment, additionally confirmed by Western blotting. Further explorations of additional aspects of the model and pharmacological agent used (EEG), as well as preliminary determinations of the plausible mechanisms mediating the observed synuclein-burden modulatory effect of SWS manipulation (mass spectrometry and immunofluorescence), were secondary assessments in the study.

The sample size used in each experiment followed the common practices of the field and was not predefined by power calculations. In vivo experiments followed termination criteria based on humane end points and animal welfare, as per animal experimentation licenses ZH205/12 and ZH210/17. Rules for stopping data collection during in vivo studies involved impairment in parameters such as weight progression, grooming, and home cage activity. Signs of pain (as per the grimace scale), discomfort, and distress were additionally monitored and documented. Dedicated score sheets [scores varying from 0 (not affected) to 3 (severely affected)] were filled in daily throughout the course of the studies. Any animal presenting a prolonged increase of any scored parameter that did not resume with appropriate management was excluded from the experiments and immediately euthanized. In the behavioral studies, mice presenting strong signs of anxiety during the testing phase and/or mathematical outliers (defined as cases with behavioral scores >2

SDs from each overall group mean) were additionally excluded from the analysis. Electrophysiological data exclusion responded to malfunction of EEG cables (with disconnection or animal bites as usual causes). The two long-term slow-wave modulation experiments followed similar end point selection criteria adapted to each model's characteristics: Long-term slow-wave modulation in VMAT2 LO mice had its end point at 18 months of age to guarantee that the 4-month-long intervention (starting at 14 months) covered the brink to synucleinopathy previously described in this model (51, 52), whereas, for the same reason, long-term slow-wave enhancement in A53T mice's end point was set at 9.5 months of age (61). Male VMAT2 animals of each genotype (WT and LO) were bred in-house, randomly allocated per genotype to the different experimental groups (P, SE, and SD) at weaning, and aged until experiments started. Male and female A53T and WT animals were purchased from The Jackson Laboratory 2 months before the start of the experiments. The allocation of the 16 WT (8 males and 8 females) and 16 A53T (8 males and 8 females) into P or SE groups was done randomly within each sex and genotype. Animal handling during the in vivo studies was performed by nonblinded experimenters, whereas automated assessment of outcomes and experimenter-performed data analysis were blinded. A variable number of mice/brains/sections/proteins/clusters ($n = 2 \geq 4000$) was analyzed in individual experiment based on availability and standard practices for the outcome of interest. The individual and specific number of replicates in each experiment is depicted in the respective figure captions and in the Supplementary Materials.

Statistics
We performed two-way analysis of variance (ANOVA), one-way ANOVA, repeated-measures ANOVA, factorial ANOVA, multivariate ANOVA, unpaired and paired one-tailed or two-tailed Student's t test, Wilcoxon signed-rank test, and post hoc analysis of Dunnett's, Fisher's, or Bonferroni's test as appropriate. All bars in the graphs represent the groups' mean, and the error bars indicate the SEM. The statistics P value is indicated in each figure legend. * indicates significant differences corresponding to P values lower than 0.05, ** corresponds to P values lower than 0.01, and *** corresponds to P values lower than 0.001.

SUPPLEMENTARY MATERIALS
www.science.org/doi/10.1126/scitranslmed.abe7099
Materials and Methods
Figs. S1 to S13
Tables S1 and S2
Data file S1
References (93–101)

View/request a protocol for this paper from *Bio-protocol*.

REFERENCES AND NOTES
1. M. J. Sateia, K. Doghramji, P. J. Hauri, C. M. Morin, Evaluation of chronic insomnia. An American Academy of Sleep Medicine review. *Sleep* **23**, 243–308 (2000).
2. D. Garcia-Borreguero, O. Larrosa, M. Bravo, Parkinson's disease and sleep. *Sleep Med. Rev.* **7**, 115–129 (2003).
3. V. C. De Cock, M. Vidailhet, I. Arnulf, Sleep disturbances in patients with parkinsonism. *Nat. Clin. Pract. Neurol.* **4**, 254–266 (2008).
4. R. B. Postuma, A. Iranzo, B. Hogl, I. Arnulf, L. Ferini-Strambi, R. Manni, T. Miyamoto, W. Oertel, Y. Dauvilliers, Y. E. Ju, M. Puligheddu, K. Sonka, A. Pelletier, J. Santamaria, B. Frauscher, S. Leu-Semenescu, M. Zucconi, M. Terzaghi, M. Miyamoto, M. M. Unger, B. Carlander, M. L. Fantini, J. Y. Montplaisir, Risk factors for neurodegeneration in idiopathic rapid eye movement sleep behavior disorder: A multicenter study. *Ann. Neurol.* **77**, 830–839 (2015).

5. J. E. Kang, M. M. Lim, R. J. Bateman, J. J. Lee, L. P. Smyth, J. R. Cirrito, N. Fujiki, S. Nishino, D. M. Holtzman, Amyloid-beta dynamics are regulated by orexin and the sleep-wake cycle. *Science* **326**, 1005–1007 (2009).

6. Y.-E. S. Ju, S. J. Ooms, C. Sutphen, S. L. Macauley, M. A. Zangrilli, G. Jerome, A. M. Fagan, E. Mignot, J. M. Zempel, J. A. H. R. Claassen, D. M. Holtzman, Slow wave sleep disruption increases cerebrospinal fluid amyloid-β levels. *Brain* **140**, 2104–2111 (2017).

7. S. Sohail, L. Yu, J. A. Schneider, D. A. Bennett, A. S. Buchman, A. S. P. Lim, Sleep fragmentation and Parkinson's disease pathology in older adults without Parkinson's disease. *Mov. Disord.* **32**, 1729–1737 (2017).

8. K. E. Sprecher, R. L. Koscik, C. M. Carlsson, H. Zetterberg, K. Blennow, O. C. Okonkwo, M. A. Sager, S. Asthana, S. C. Johnson, R. M. Benca, B. B. Bendlin, Poor sleep is associated with CSF biomarkers of amyloid pathology in cognitively normal adults. *Neurology* **89**, 445–453 (2017).

9. B. P. Lucey, T. J. Hicks, J. S. McLeland, C. D. Toedebusch, J. Boyd, D. L. Elbert, B. W. Patterson, J. Baty, J. C. Morris, V. Ovod, K. G. Mawuenyega, R. J. Bateman, Effect of sleep on overnight cerebrospinal fluid amyloid β kinetics. *Ann. Neurol.* **83**, 197–204 (2018).

10. J. H. Roh, Y. Huang, A. W. Bero, T. Kasten, F. R. Stewart, R. J. Bateman, D. M. Holtzman, Disruption of the sleep-wake cycle and diurnal fluctuation of β-amyloid in mice with Alzheimer's disease pathology. *Sci. Transl. Med.* **4**, 150ra122 (2012).

11. A. Videnovic, E. B. Klerman, W. Wang, A. Marconi, T. Kuhta, P. C. Zee, Timed light therapy for sleep and daytime sleepiness associated with Parkinson disease: A randomized clinical trial. *JAMA Neurol.* **74**, 411–418 (2017).

12. F. Buchele, M. Hackius, S. R. Schreglmann, W. Omlor, E. Werth, A. Maric, L. L. Imbach, S. Hägele-Link, D. Waldvogel, Sodium oxybate for excessive daytime sleepiness and sleep disturbance in Parkinson disease: A randomized clinical trial. *JAMA Neurol.* **75**, 114–118 (2018).

13. S. J. Schreiner, L. L. Imbach, E. Werth, R. Poryazova, H. Baumann-Vogel, P. O. Valko, T. Murer, D. Noain, C. R. Baumann, Slow-wave sleep and motor progression in Parkinson disease. *Ann. Neurol.* **85**, 765–770 (2019).

14. G. Ringstad, S. A. S. Vatnehol, P. K. Eide, Glymphatic MRI in idiopathic normal pressure hydrocephalus. *Brain* **140**, 2691–2705 (2017).

15. V. Kiviniemi, X. Wang, V. Korhonen, T. Keinänen, T. Tuovinen, J. Autio, P. LeVan, S. Keilholz, Y. F. Zang, J. Hennig, M. Nedergaard, Ultra-fast magnetic resonance encephalography of physiological brain activity–Glymphatic pulsation mechanisms? *J. Cereb. Blood Flow Metab.* **36**, 1033–1045 (2016).

16. L. Xie, H. Kang, Q. Xu, M. J. Chen, Y. Liao, M. Thiyagarajan, J. O'Donnell, D. J. Christensen, C. Nicholson, J. J. Iliff, T. Takano, R. Deane, M. Nedergaard, Sleep drives metabolite clearance from the adult brain. *Science* **342**, 373–377 (2013).

17. N. E. Fultz, G. Bonmassar, K. Setsompop, R. A. Stickgold, B. R. Rosen, J. R. Polimeni, L. D. Lewis, Coupled electrophysiological, hemodynamic, and cerebrospinal fluid oscillations in human sleep. *Science* **366**, 628–631 (2019).

18. L. M. Hablitz, H. S. Vinitsky, Q. Sun, F. F. Stæger, B. Sigurdsson, K. N. Mortensen, T. O. Lilius, M. Nedergaard, Increased glymphatic influx is correlated with high EEG delta power and low heart rate in mice under anesthesia. *Sci. Adv.* **5**, eaav5447 (2019).

19. A. Bergel, T. Deffieux, C. Demene, M. Tanter, I. Cohen, Local hippocampal fast gamma rhythms precede brain-wide hyperemic patterns during spontaneous rodent REM sleep. *Nat. Commun.* **9**, 5364 (2018).

20. K. L. Turner, K. W. Gheres, E. A. Proctor, P. J. Drew, Neurovascular coupling and bilateral connectivity during NREM and REM sleep. *eLife* **9**, e62071 (2020).

21. N. L. Hauglund, C. Pavan, M. Nedergaard, Cleaning the sleeping brain—The potential restorative function of the glymphatic system. *Curr. Opin. Physiol.* **15**, 1–6 (2020).

22. N. Naidoo, Cellular stress/the unfolded protein response: Relevance to sleep and sleep disorders. *Sleep Med. Rev.* **13**, 195–204 (2009).

23. J. R. Cirrito, K. A. Yamada, M. B. Finn, R. S. Sloviter, K. R. Bales, P. C. May, D. D. Schoepp, S. M. Paul, S. Mennerick, D. M. Holtzman, Synaptic activity regulates interstitial fluid amyloid-beta levels in vivo. *Neuron* **48**, 913–922 (2005).

24. A. R. Saha, N. N. Ninkina, D. P. Hanger, B. H. Anderton, A. M. Davies, V. L. Buchman, Induction of neuronal death by α-synuclein. *Eur. J. Neurosci.* **12**, 3073–3077 (2000).

25. M. R. Cookson, α-Synuclein and neuronal cell death. *Mol. Neurodegener.* **4**, 9 (2009).

26. G. E. Alexander, M. D. Crutcher, Functional architecture of basal ganglia circuits: Neural substrates of parallel processing. *Trends Neurosci.* **13**, 266–271 (1990).

27. M. R. DeLong, T. Wichmann, Circuits and circuit disorders of the basal ganglia. *Arch. Neurol.* **64**, 20–24 (2007).

28. J. Jankovic, Parkinson's disease: Clinical features and diagnosis. *J. Neurol. Neurosurg. Psychiatry* **79**, 368–376 (2008).

29. H. Braak, K. D. Tredici, U. Rüb, R. A. I. de Vos, E. N. H. Jansen Steur, E. Braak, Staging of brain pathology related to sporadic Parkinson's disease. *Neurobiol. Aging* **24**, 197–211 (2003).

30. Y. C. Wong, D. Krainc, α-Synuclein toxicity in neurodegeneration: Mechanism and therapeutic strategies. *Nat. Med.* **23**, 1–13 (2017).

31. H.-J. Lee, E.-J. Bae, S.-J. Lee, Extracellular α-synuclein—A novel and crucial factor in Lewy body diseases. *Nat. Rev. Neurol.* **10**, 92–98 (2014).

32. W. Dauer, S. Przedborski, Parkinson's disease: Mechanisms and models. *Neuron* **39**, 889–909 (2003).

33. J. W. Steele, S. Ju, M. L. Lachenmayer, J. Liken, A. Stock, S. H. Kim, L. M. Delgado, I. E. Alfaro, S. Bernales, G. Verdile, P. Bharadwaj, V. Gupta, R. Barr, A. Friss, G. Dolios, R. Wang, D. Ringe, A. A. Protter, R. N. Martins, M. E. Ehrlich, Z. Yue, G. A. Petsko, S. Gandy, Latrepirdine stimulates autophagy and reduces accumulation of α-synuclein in cells and in mouse brain. *Mol. Psychiatry* **18**, 882–888 (2013).

34. M. A. Rahman, H. Rhim, Therapeutic implication of autophagy in neurodegenerative diseases. *BMB Rep.* **50**, 345–354 (2017).

35. J. J. Iliff, H. Lee, M. Yu, T. Feng, J. Logan, M. Nedergaard, H. Benveniste, Brain-wide pathway for waste clearance captured by contrast-enhanced MRI. *J. Clin. Invest.* **123**, 1299–1309 (2013).

36. N. A. Jessen, A. S. F. Munk, I. Lundgaard, M. Nedergaard, The glymphatic system: A beginner's guide. *Neurochem. Res.* **40**, 2583–2599 (2015).

37. J. M. Tarasoff-Conway, R. O. Carare, R. S. Osorio, L. Glodzik, T. Butler, E. Fieremans, L. Axel, H. Rusinek, C. Nicholson, B. V. Zlokovic, B. Frangione, K. Blennow, J. Ménard, H. Zetterberg, T. Wisniewski, M. J. de Leon, Clearance systems in the brain—Implications for Alzheimer disease. *Nat. Rev. Neurol.* **11**, 457–470 (2015).

38. S. Sundaram, R. L. Hughes, E. Peterson, E. M. Müller-Oehring, H. M. Brontë-Stewart, K. L. Poston, A. Faerman, C. Bhowmick, T. Schulte, Establishing a framework for neuropathological correlates and glymphatic system functioning in Parkinson's disease. *Neurosci. Biobehav. Rev.* **103**, 305–315 (2019).

39. J. K. Holth, S. K. Fritschi, C. Wang, N. P. Pedersen, J. R. Cirrito, T. E. Mahan, M. B. Finn, M. Manis, J. C. Geerling, P. M. Fuller, B. P. Lucey, D. M. Holtzman, The sleep-wake cycle regulates brain interstitial fluid tau in mice and CSF tau in humans. *Science* **363**, 880–884 (2019).

40. N. R. Barthélémy, H. Liu, W. Lu, P. T. Kotzbauer, R. J. Bateman, B. P. Lucey, Sleep deprivation affects tau phosphorylation in human cerebrospinal fluid. *Ann. Neurol.* **87**, 700–709 (2020).

41. T. C. Wetter, V. Collado-Seidel, T. Pollmacher, A. Yassouridis, C. Trenkwalder, Sleep and periodic leg movement patterns in drug-free patients with Parkinson's disease and multiple system atrophy. *Sleep* **23**, 361–367 (2000).

42. M. Wienecke, E. Werth, R. Poryazova, H. Baumann-Vogel, C. L. Bassetti, M. Weller, D. Waldvogel, A. Storch, C. R. Baumann, Progressive dopamine and hypocretin deficiencies in Parkinson's disease: Is there an impact on sleep and wakefulness? *J. Sleep Res.* **21**, 710–717 (2012).

43. R. B. Postuma, D. Aarsland, P. Barone, D. J. Burn, C. H. Hawkes, W. Oertel, T. Ziemssen, Identifying prodromal Parkinson's disease: Pre-motor disorders in Parkinson's disease. *Mov. Disord.* **27**, 617–626 (2012).

44. M. Moazami-Goudarzi, J. Sarnthein, L. Michels, R. Moukhtieva, D. Jeanmonod, Enhanced frontal low and high frequency power and synchronization in the resting EEG of parkinsonian patients. *Neuroimage* **41**, 985–997 (2008).

45. D. Petit, J. F. Gagnon, M. L. Fantini, L. Ferini-Strambi, J. Montplaisir, Sleep and quantitative EEG in neurodegenerative disorders. *J. Psychosom. Res.* **56**, 487–496 (2004).

46. D. M. Robinson, G. M. Keating, Sodium oxybate: A review of its use in the management of narcolepsy. *CNS Drugs* **21**, 337–354 (2007).

47. M. M. Morawska, F. Buchele, C. G. Moreira, L. L. Imbach, D. Noain, C. R. Baumann, Sleep modulation alleviates axonal damage and cognitive decline after rodent traumatic brain injury. *J. Neurosci.* **36**, 3422–3429 (2016).

48. R. Huber, T. Deboer, I. Tobler, Sleep deprivation in prion protein deficient mice sleep deprivation in prion protein deficient mice and control mice: Genotype dependent regional rebound. *Neuroreport* **13**, 1–4 (2002).

49. N. L. Hauglund, P. Kusk, B. R. Kornum, M. Nedergaard, Meningeal lymphangiogenesis and enhanced glymphatic activity in mice with chronically implanted EEG electrodes. *J. Neurosci.* **40**, 2371–2380 (2020).

50. D. P. Brunner, D. J. Dijk, I. Tobler, A. A. Borbely, Effect of partial sleep deprivation on sleep stages and EEG power spectra: Evidence for non-REM and REM sleep homeostasis. *Electroencephalogr. Clin. Neurophysiol.* **75**, 492–499 (1990).

51. W. M. Caudle, J. R. Richardson, M. Z. Wang, T. N. Taylor, T. S. Guillot, A. L. McCormack, R. E. Colebrooke, D. A. di Monte, P. C. Emson, G. W. Miller, Reduced vesicular storage of dopamine causes progressive nigrostriatal neurodegeneration. *J. Neurosci.* **27**, 8138–8148 (2007).

52. T. N. Taylor, W. M. Caudle, G. W. Miller, VMAT2-deficient mice display nigral and extranigral pathology and motor and nonmotor symptoms of Parkinson's disease. *Parkinsons Dis.* **2011**, 124165 (2011).

53. K. B. Franklin, G. Paxinos, *Paxinos and Franklin's the Mouse Brain in Stereotaxic Coordinates, Compact: The Coronal Plates and Diagrams* (Academic Press, 2019).

54. H. Fujiwara, M. Hasegawa, N. Dohmae, A. Kawashima, E. Masliah, M. S. Goldberg, J. Shen, K. Takio, T. Iwatsubo, α-Synuclein is phosphorylated in synucleinopathy lesions. *Nat. Cell Biol.* **4**, 160–164 (2002).

Morawska *et al.*, *Sci. Transl. Med.* **13**, eabe7099 (2021)   8 December 2021

11 of 13

55. H. J. Rideout, P. Dietrich, Q. Wang, W. T. Dauer, L. Stefanis, α-Synuclein is required for the fibrillar nature of ubiquitinated inclusions induced by proteasomal inhibition in primary neurons. *J. Biol. Chem.* **279**, 46915–46920 (2004).

56. L. Chen, M. B. Feany, α-Synuclein phosphorylation controls neurotoxicity and inclusion formation in a *Drosophila* model of Parkinson disease. *Nat. Neurosci.* **8**, 657–663 (2005).

57. K. Beyer, A. Ariza, Alpha-Synuclein posttranslational modification and alternative splicing as a trigger for neurodegeneration. *Mol. Neurobiol.* **47**, 509–524 (2013).

58. K. J. Spinelli, J. K. Taylor, V. R. Osterberg, M. J. Churchill, E. Pollock, C. Moore, C. K. Meshul, V. K. Unni, Presynaptic alpha-synuclein aggregation in a mouse model of Parkinson's disease. *J. Neurosci.* **34**, 2037–2050 (2014).

59. M. L. Kramer, C. Behrens, W. J. Schulz-Schaeffer, Selective detection, quantification, and subcellular location of α-synuclein aggregates with a protein aggregate filtration assay. *Biotechniques* **44**, 403–411 (2008).

60. A. L. McCormack, S. K. Mak, D. A. Di Monte, Increased α-synuclein phosphorylation and nitration in the aging primate substantia nigra. *Cell Death Dis.* **3**, e315 (2012).

61. B. I. Giasson, J. E. Duda, S. M. Quinn, B. Zhang, J. Q. Trojanowski, V. M. Y. Lee, Neuronal alpha-synucleinopathy with severe movement disorder in mice expressing A53T human alpha-synuclein. *Neuron* **34**, 521–533 (2002).

62. J. J. Iliff, M. Wang, Y. Liao, B. A. Plogg, W. Peng, G. A. Gundersen, H. Benveniste, G. E. Vates, R. Deane, S. A. Goldman, E. A. Nagelhus, M. Nedergaard, A paravascular pathway facilitates CSF flow through the brain parenchyma and the clearance of interstitial solutes, including amyloid beta. *Sci. Transl. Med.* **4**, 147ra111 (2012).

63. D. M. Zeppenfeld, M. Simon, J. D. Haswell, C. D'Abreo, C. Murchison, J. F. Quinn, M. R. Grafe, R. L. Woltjer, J. Kaye, J. J. Iliff, Association of perivascular localization of aquaporin-4 with cognition and Alzheimer disease in aging brains. *JAMA Neurol.* **74**, 91–99 (2017).

64. K. A. Mooslehner, P. M. Chan, W. Xu, L. Liu, C. Smadja, T. Humby, N. D. Allen, L. S. Wilkinson, P. C. Emson, Mice with very low expression of the vesicular monoamine transporter 2 gene survive into adulthood: Potential mouse model for parkinsonism. *Mol. Cell. Biol.* **21**, 5321–5331 (2001).

65. B. Högl, A. Stefani, A. Videnovic, Idiopathic REM sleep behaviour disorder and neurodegeneration—An update. *Nat. Rev. Neurol.* **14**, 40–55 (2018).

66. M. D. Gjerstad, T. Wentzel-Larsen, D. Aarsland, J. P. Larsen, Insomnia in Parkinson's disease: Frequency and progression over time. *J. Neurol. Neurosurg. Psychiatry* **78**, 476–479 (2007).

67. B. Platt, B. Drever, D. Koss, S. Stoppelkamp, A. Jyoti, A. Plano, A. Utan, G. Merrick, D. Ryan, V. Melis, H. Wan, M. Mingarelli, E. Porcu, L. Scrocchi, A. Welch, G. Riedel, Abnormal cognition, sleep, EEG and brain metabolism in a novel knock-in Alzheimer mouse, PLB1. *PLOS ONE* **6**, e27068 (2011).

68. S. Kantor, J. Varga, S. Kulkarni, A. J. Morton, Chronic paroxetine treatment prevents the emergence of abnormal electroencephalogram oscillations in Huntington's disease mice. *Neurotherapeutics* **14**, 1120–1133 (2017).

69. J. Hlinka, C. Alexakis, A. Diukova, P. F. Liddle, D. P. Auer, Slow EEG pattern predicts reduced intrinsic functional connectivity in the default mode network: An inter-subject analysis. *Neuroimage* **53**, 239–246 (2010).

70. L. M. Hablitz, V. Plá, M. Giannetto, H. S. Vinitsky, F. F. Stæger, T. Metcalfe, R. Nguyen, A. Benrais, M. Nedergaard, Circadian control of brain glymphatic and lymphatic fluid flow. *Nat. Commun.* **11**, 4411 (2020).

71. E. S. Musiek, D. M. Holtzman, Mechanisms linking circadian clocks, sleep, and neurodegeneration. *Science* **354**, 1004–1008 (2016).

72. S. M. Abbott, A. Videnovic, Chronic sleep disturbance and neural injury: Links to neurodegenerative disease. *Nat. Sci. Sleep* **8**, 55–61 (2016).

73. M. Nedergaard, S. A. Goldman, Glymphatic failure as a final common pathway to dementia. *Science* **370**, 50–56 (2020).

74. G. Costa, M. J. Sisalli, N. Simola, S. Della Notte, M. A. Casu, M. Serra, A. Pinna, A. Feliciello, L. Annunziato, A. Scorziello, M. Morelli, Gender differences in neurodegeneration, neuroinflammation and Na$^+$-Ca2$^+$ exchangers in the female A53T transgenic mouse model of Parkinson's disease. *Front. Aging Neurosci.* **12**, 118 (2020).

75. C. Gakuba, T. Gaberel, S. Goursaud, J. Bourges, C. di Palma, A. Quenault, S. M. de Lizarrondo, D. Vivien, M. Gauberti, General anesthesia inhibits the activity of the "glymphatic system". *Theranostics* **8**, 710–722 (2018).

76. N. F. Bence, R. M. Sampat, R. R. Kopito, Impairment of the ubiquitin-proteasome system by protein aggregation. *Science* **292**, 1552–1555 (2001).

77. K. S. P. McNaught, C. W. Olanow, B. Halliwell, O. Isacson, P. Jenner, Failure of the ubiquitin–proteasome system in Parkinson's disease. *Nat. Rev. Neurosci.* **2**, 589–594 (2001).

78. A. L. Goldberg, Protein degradation and protection against misfolded or damaged proteins. *Nature* **426**, 895–899 (2003).

79. C. Soto, Unfolding the role of protein misfolding in neurodegenerative diseases. *Nat. Rev. Neurosci.* **4**, 49–60 (2003).

80. H. J. Lee, S. Patel, S. J. Lee, Intravesicular localization and exocytosis of alpha-synuclein and its aggregates. *J. Neurosci.* **25**, 6016–6024 (2005).

81. M. T. Lin, M. F. Beal, Mitochondrial dysfunction and oxidative stress in neurodegenerative diseases. *Nature* **443**, 787–795 (2006).

82. D. C. Rubinsztein, The roles of intracellular protein-degradation pathways in neurodegeneration. *Nature* **443**, 780–786 (2006).

83. P. J. Khandelwal, S. B. Dumanis, L. R. Feng, K. Maguire-Zeiss, G. W. Rebeck, H. A. Lashuel, C. E. H. Moussa, Parkinson-related parkin reduces α-synuclein phosphorylation in a gene transfer model. *Mol. Neurodegener.* **5**, 47 (2010).

84. Y. He, G. G. Cornelissen-Guillaume, J. He, A. J. Kastin, L. M. Harrison, W. Pan, Circadian rhythm of autophagy proteins in hippocampus is blunted by sleep fragmentation. *Chronobiol. Int.* **33**, 553–560 (2016).

85. F. Brüning, S. B. Noya, T. Bange, S. Koutsouli, J. D. Rudolph, S. K. Tyagarajan, J. Cox, M. Mann, S. A. Brown, M. S. Robles, Sleep-wake cycles drive daily dynamics of synaptic phosphorylation. *Science* **366**, eaav3617 (2019).

86. D. J. Taylor, K. L. Lichstein, H. H. Durrence, Insomnia as a health risk factor. *Behav. Sleep Med.* **1**, 227–247 (2003).

87. P. Jennum, R. Ibsen, K. Avlund, J. Kjellberg, Health, social and economic consequences of hypersomnia: A controlled national study from a national registry evaluating the societal effect on patients and their partners. *Eur. J. Health Econ.* **15**, 303–311 (2014).

88. J. Zhou, M. Broe, Y. Huang, J. P. Anderson, W. P. Gai, E. A. Milward, M. Porritt, D. Howells, A. J. Hughes, X. Wang, G. M. Halliday, Changes in the solubility and phosphorylation of α-synuclein over the course of Parkinson's disease. *Acta Neuropathol.* **121**, 695–704 (2011).

89. F. Blandini, M. T. Armentero, Animal models of Parkinson's disease. *FEBS J.* **279**, 1156–1166 (2012).

90. R. B. Machado, D. Suchecki, S. Tufik, Comparison of the sleep pattern throughout a protocol of chronic sleep restriction induced by two methods of paradoxical sleep deprivation. *Brain Res. Bull.* **70**, 213–220 (2006).

91. H.-V. Ngo, T. Martinetz, J. Born, M. Molle, Auditory closed-loop stimulation of the sleep slow oscillation enhances memory. *Neuron* **78**, 545–553 (2013).

92. L. Besedovsky, H. V. V. Ngo, S. Dimitrov, C. Gassenmaier, R. Lehmann, J. Born, Auditory closed-loop stimulation of EEG slow oscillations strengthens sleep and signs of its immune-supportive function. *Nat. Commun.* **8**, 1984 (2017).

93. J. T. Lettieri, H. L. Fung, Dose-dependent pharmacokinetics and hypnotic effects of sodium gamma-hydroxybutyrate in the rat. *J. Pharmacol. Exp. Ther.* **208**, 7–11 (1979).

94. F. Nava, G. Carta, M. Bortolato, G. L. Gessa, γ-Hydroxybutyric acid and baclofen decrease extracellular acetylcholine levels in the hippocampus via GABA$_B$ receptors. *Eur. J. Pharmacol.* **430**, 261–263 (2001).

95. E. J. van Rooden, B. I. Florea, H. Deng, M. P. Baggelaar, A. C. M. van Esbroeck, J. Zhou, H. S. Overkleeft, M. van der Stelt, Mapping in vivo target interaction profiles of covalent inhibitors using chemical proteomics with label-free quantification. *Nat. Protoc.* **13**, 752–767 (2018).

96. D. W. Huang, B. T. Sherman, R. A. Lempicki, Systematic and integrative analysis of large gene lists using DAVID bioinformatics resources. *Nat. Protoc.* **4**, 44–57 (2009).

97. D. W. Huang, B. T. Sherman, R. A. Lempicki, Bioinformatics enrichment tools: Paths toward the comprehensive functional analysis of large gene lists. *Nucleic Acids Res.* **37**, 1–13 (2009).

98. S. Babicki, D. Arndt, A. Marcu, Y. Liang, J. R. Grant, A. Maciejewski, D. S. Wishart, Heatmapper: Web-enabled heat mapping for all. *Nucleic Acids Res.* **44**, W147–W153 (2016).

99. I. Tobler, T. Deboer, M. Fischer, Sleep and sleep regulation in normal and prion protein-deficient mice. *J. Neurosci.* **17**, 1869–1879 (1997).

100. D. Noain, F. Büchele, S. R. Schreglmann, P. O. Valko, Y. V. Gavrilov, M. M. Morawska, L. L. Imbach, C. R. Baumann, Increased sleep need and reduction of tuberomammillary histamine neurons after rodent traumatic brain injury. *J. Neurotrauma* **35**, 85–93 (2018).

101. E. Werth, D. J. Dijk, P. Achermann, A. A. Borbely, Dynamics of the sleep EEG after an early evening nap: Experimental data and simulations. *Am. J. Physiol.* **271**, R501–R510 (1996).

Morawska *et al.*, *Sci. Transl. Med.* **13**, eabe7099 (2021)   8 December 2021

12 of 13

Morawska *et al.*, *Sci. Transl. Med.* **13**, eabe7099 (2021)   8 December 2021

13 of 13

Science Translational Medicine

Slow-wave sleep affects synucleinopathy and regulates proteostatic processes in mouse models of Parkinson's disease

Marta M. MorawskaCarlos G. MoreiraVarun R. GindePhilipp O. ValkoTobias WeissFabian BücheleLukas L. ImbachSophie MasneufSedef KollarikNatalia PrymaczokJuan A. GerezRoland RiekChristian R. BaumannDaniela Noain

Sleep for Parkinson's

Sleep disturbances have been shown to occur and to contribute to several neurodegenerative diseases, including Parkinson's disease (PD). In particular, slow-wave sleep (SWS) alterations show correlation with PD symptoms and progression. Here, Morawska *et al.* investigated the relationship between SWS alterations and #-synuclein (#Syn) deposition in rodent models of PD. Sleep deprivation increased brain #Syn aggregates, whereas enhancing SWS with sodium oxybate reduced #Syn burden, possibly by increasing glymphatic function and modulating protein homeostasis. The results suggest that sleep plays an important role in PD pathophysiology and that manipulating SWS might be therapeutic in patients with PD.

View the article online
https://www.science.org/doi/10.1126/scitranslmed.abe7099
Permissions
https://www.science.org/help/reprints-and-permissions